Adapting gas-phase electron scattering *R*-matrix calculations to a condensed-matter environment

Laurent Caron,* D. Bouchiha, J. D. Gorfinkiel,† and L. Sanche
[1]*Groupe de Recherches en Sciences des Radiations, Faculté de médecine, Université de Sherbrooke, Sherbrooke, QC J1H 5N4, Canada*
(Received 25 January 2007; revised manuscript received 20 June 2007; published 28 September 2007)

We investigate how gas phase *R*-matrix calculations for electron collisions with the water molecule can be efficiently used in a condensed environment. The electron band structure of cubic ice being fairly well studied, we try to reproduce it using a generalization of the Korringa-Kohn-Rostoker band calculation method. We find two cutoffs have to be applied to the *R*-matrix elastic scattering results in condensed matter: one on the range of the molecular dipole and another in the angular momentum components of the scattering matrix. Their origins and physical meaning are discussed.

DOI: 10.1103/PhysRevA.76.032716 PACS number(s): 34.80.Bm, 71.20.−b, 87.64.Bx

I. INTRODUCTION

Understanding the interaction of low energy electrons (LEEs) ($E \lesssim 30$ eV) in condensed matter is a subject of fundamental importance that finds applications in such diverse fields as radiation chemistry [1,2] and biology [3], beam- and photon-induced surface chemistry [4–8], space planetology [9], and dielectric aging [10]. These applications often require that the cross sections (CSs) involved in particular condensed phase processes be known in order to evaluate and predict the effects of low-energy electron interactions. Such CSs have to be obtained experimentally for specific conditions that vary according to the nature of the condensed system, its state of aggregation and the type of interfaces between different media. To avoid performing an experiment for each particular case, it would be highly desirable to use a theoretical framework that would allow one to generate condensed phase CSs or transform those obtained in the gas-phase to condensed phase values by the inclusion of suitable parameters. Unfortunately, these types of formulation, which should include multiple electron scattering outside the target molecule, are not presently available. Nevertheless, attempts have been made to achieve this goal.

Lekner [11] first showed that, within the Born approximation, condensed-phase electron scattering CS could be derived from the product of the gas-phase CS and the structure factor of the solid. Much later, Fabrikant *et al.* [12–15] evaluated dissociative electron attachment CS for halo- and fluorohalo-carbons in the bulk of rare gas solids from *R*-matrix calculations in which solid Kr was represented by including the polarization energy and the electron's effective mass, but not the full band structure (e.g., the K-dispersion relation). Comparison between experimental and theoretical CS allowed them to analyze the gas-phase parameters that must be modified to generate condensed-phase CS from gas-phase data.

The *R*-matrix is a powerful *ab initio* method for calculating electron-molecule scattering information [16,17] in the gas phase. Its use in a condensed matter context, however, is far from routine. In addition to the works on dissociative electron attachment [12–15] mentioned previously, there have been studies of inelastic scattering [18,19] from molecules adsorbed on surfaces or in the bulk of rare gas solids at low energy. These have used a continuum treatment of the substrate or bulk. More recently, a microscopic cluster treatment of inelastic scattering by a molecule in a host medium has been carried out [20]. This was done at the expense of using a large angular momentum basis $l \leq 30$ for the spherical harmonics describing the cluster. It would be interesting to have a more computationally economical, yet microscopic, approach in the condensed phase built on multiple scattering between independent units, where each of these are described by *R*-matrix data. This would be very useful, for instance, in Monte Carlo electron transport calculations at low energy [21].

In the present article, we propose a framework based on the *R*-matrix theory to describe LEE scattering from a molecule embedded in a solid. We use the H_2O molecule and its cubic ice phase as a model system. On the one hand, water is an important biological liquid [22] for which scattering data is crucial. On the other hand, the electron band structure of the cubic phase of ice has been extensively studied [23–25]. Although we shall be doing a band structure calculation of ice using the Korringa-Kohn-Rostoker (KKR) method, our objective is not to do yet another computation of the bands. Rather, our aim is to provide a calibration reference which will guide us in the choice of constraints to impose on the gas phase *R*-matrix elastic scattering results for the study of scattering from ice.

We shall first describe the essentials of the *R*-matrix theory. This will be followed by a presentation of the KKR method with an effort to link it to its multiple scattering equivalent approach. We shall then present the results of our numerical calculations and extract guidelines in the use of the *R*-matrix within a condensed environment.

II. R-MATRIX

A brief description of the *R*-matrix method as applied within the fixed-nuclei approximation is as follows. The method is based on splitting coordinate space into two re-

*Permanent address: Département de physique et Regroupement québécois sur les matériaux de pointe, Université de Sherbrooke, Sherbrooke, QC J1K 2R1, Canada.
†Department of Physics and Astronomy, The Open University, Walton Hall, MK7 6AA Milton Keynes, UK.

gions separated by a sphere of radius a, which we shall henceforth call the R sphere, centered on the center of mass of the molecule. The dominant electron-molecule interactions are different in these two regions and can therefore be treated differently. Inside the R sphere the incident electron lies within the molecular electron cloud. Thus, both the exchange and electron-electron correlation are significant and must be taken into account. The wave functions for the description of the N-electron target + scattering electron system are expanded in the following way:

$$\Psi_k^{N+1} = \mathcal{A}\sum_{ij} a_{ijk}\phi_i(x_1, \ldots, x_N)u_{ij}(x_{N+1}) + \sum_i b_{ik}\chi_i(x_1, \ldots, x_{N+1}), \quad (1)$$

where $\mathcal{A}$ is the antisymmetrization operator, $u_{ij}(x_i)$ are continuum orbitals describing the scattering electron and x_i are the spatial and spin coordinates of electron i; ϕ_i are target wave functions and χ_i are known as L^2 functions. These χ_i are multicenter quadratically integrable functions constructed from the target occupied and virtual molecular orbitals (MOs) and are used to represent short range correlation and polarization effects.

The target wave functions are normally obtained using the configuration interaction (CI) method. The configurations included in the expansion are generated as products of MOs. To ensure a good balance between the target and $N+1$ description, a complete active space configuration interaction (CASCI) model for the target description is chosen. In it all excitations are performed among a set of orbitals, the active space, that normally span the valence space of the target. In the polyatomic R-matrix suite [26], both the molecular and the continuum orbitals $u_{ij}(x_i)$ are expanded in terms of Gaussian-type orbitals (GTOs). The basis functions for the MOs, centered on each nuclei, are normally adapted from standard quantum chemistry basis sets. The "continuum" GTOs are centered at the center of mass of the system and generated using the program GTOBAS [27].

In the outer region, exchange and correlation are negligible and the electron-target interaction is described in terms of a long-range multipolar expansion. To obtain the wave functions describing the system, a set of coupled single-center differential equations are solved by propagating the R-matrix to a region where the electron-molecule interaction can be considered negligible [17]. In the limit $r \to \infty$, the differential equations have j different, linearly independent asymptotic solutions for each energetically open channel i [17]:

$$F_{ij}(r) \sim k_i^{-1/2}(\sin\theta_i\delta_{ij} + \cos\theta_i K_{ij}), \quad (2)$$

where $\theta_i = k_i r - \frac{1}{2}l_i\pi$, k_i expresses the difference between the total energy of the system and the eigenenergy of the corresponding target state and l_i are the channel angular momenta. The K matrix defined by K_{ij} contains all the information needed to derive the scattering observables such as the elastic cross section.

For an accurate description of the water molecule we have used the UK polyatomic R-matrix code [26] and followed the work by Gorfinkiel *et al.* [28]. However, in this work, only the ground state has been included in the close-coupling expansion. For the target description we used the double-zeta plus polarization (DZP) Gaussian basis set for O [29] and the triple-zeta (TZ) basis for H [30]. In contrast to Ref. [28], no diffuse functions were added: (1) in order to keep the size of the R sphere small for compatibility with the muffin-tin theory and (2) we limited our calculation to the ground state; the diffuse functions were needed in Ref. [28] mainly to improve the description of the excited states. The same procedure for generating the pseudonatural orbitals (NOs) and the same CASCI model as in Ref. [28] were used. The resulting ground state energy is −76.108 Hartree and the dipole moment, 0.7687 a.u. The latter is slightly higher with our compact basis set (although still only 5% higher than the experimental value) but the ground-state energy is very similar to the one obtained in Ref. [28]; both are in good agreement with other published data.

The radius of the R-sphere must be chosen in such a way that all the electronic density of the state included in the calculation is negligible outside it. Using a compact basis set allowed us to test smaller R-matrix radii than $a=10$ a.u, the one used in Ref. [28]. The final calculations were carried out with a radius of $a=6$ a.u. Special care was taken to verify that the sphere contained all the electronic density. The partial wave expansion was initially limited to $l \leq 4$ as in Ref. [28]. The elastic cross section calculated with our model and that of Ref. [28] agreed very well. For the present study, we calculate the required K matrix by removing the dipole contribution outside the R-sphere.

III. KKR

The R-matrix, which confines the detailed physics description within its R sphere, is in principle, well suited to a multiple scattering approach of the muffin-tin-type used in solid state theory [31] and recently proposed for macromolecules [32–34]. In the KKR, the scatterers sit in the muffin cavities and bathe in a constant potential energy V_0 also filling the space between muffins. V_0 is of order of the polarization energy seen by an electron between the muffins. The KKR method is well suited to a band theoretical calculation [35] of centrosymmetric molecules. As Segall and Ham [35] mention in their Sec. IV, the method might be expected to behave poorly in more complex situations such as those with two atoms per unit cell as in the diamond structure. Calculations in such cases, however, turn out to be quite good. That is the reason why we initially believed the KKR might prove appropriate even for molecules with a dipole, such as H_2O. Let us now review the theory.

A. One scatterer per unit cell

1. Simple centrosymmetric atoms

The Bloch eigenmodes for an infinite crystal are determined by the nontrivial solutions of a set of coupled linear equations for the angular momentum amplitudes at the sur-

face of the muffin tins. Consequently, the determinant of the coefficient matrix is zero for those solutions. Bloch's theorem imposes translational symmetry throughout the crystal. This zero determinant search, for molecules described by phase shifts, is expressed as [31]

$$|\bar{\Gamma}_{LL'} + \kappa\delta_{LL'}\cot(\delta_l)| = 0, \tag{3}$$

where $L=(l,m)$, $\kappa=\sqrt{E}$, E is the kinetic energy of the electron (here in Ryd) relative to V_0, δ_l is the phase shift,

$$\bar{\Gamma}_{LL'} = 4\pi i^{l-l'}\sum_{L_1} i^{-l_1} D_{L_1} C_{L_1,L,L'}, \tag{4}$$

$C_{L_1,L,L'}=\int d\Omega Y_L^*(\Omega)Y_{L'}(\Omega)Y_{L_1}(\Omega)$, and Y_L is a spherical harmonic. The quantities $D_{L_1}(\vec{k},E)$ depend on the crystal structure as well as the wave vector $\vec{k}$ and the energy E of the electron. Their expression is

$$D_{L_1} = D_{L_1}^{(1)} + D_{L_1}^{(2)} + D_0^{(3)}\delta_{L_1 0} \tag{5}$$

with

$$D_{L_1}^{(1)} = \frac{4\pi}{\Omega_m}\frac{i^{l_1}}{\kappa^{l_1}}\sum_p \frac{k_p^{l_1} Y_{L_1}^*(\hat{k}_p)}{\kappa^2 - k_p^2}\exp[(\kappa^2 - k_p^2)/\eta], \tag{6}$$

$$D_{L_1}^{(2)} = -\pi^{-1/2}\frac{2^{l_1+1}}{\kappa^{l_1}}\sum_{n\neq 0} e^{i\vec{k}\cdot\vec{A}_n}|\vec{A}_n|^{l_1} Y_{L_1}^*(\hat{A}_n)\int_{\sqrt{\eta}/2}^{\infty} d\xi\xi^{2l_1} \times\exp\left[-\xi^2|\vec{A}_n|^2 + \frac{\kappa^2}{4\xi^2}\right], \tag{7}$$

$$D_0^{(3)} = -\frac{\sqrt{\eta}}{2\pi}\sum_{s=0}^{\infty}\frac{(\kappa^2/\eta)^s}{s!\,(2s-1)}, \tag{8}$$

where η is a convergence factor for the sums over the lattice vectors $(\vec{A}_n)$ and the reciprocal lattice $(\vec{K}_p)$, $\vec{k}_p=\vec{K}_p+\vec{k}$, $\vec{k}$ is the Bloch wave vector, and Ω_m is the volume of the unit cell. We have used the value $\eta=8\pi/a_l^2$, where a_l is the fcc lattice parameter of cubic ice. This value of η is used in similar sums appearing in the theory of low-energy electron diffraction (LEED) [38]. The value of D_{L_1} is independent of the exact value of η.

2. Link to multiple scattering theory

The formalism developed by Caron and Sanche [33] for multiple scattering, proposes the self-consistent relation

$$i^l B_L^{(n)} = \sum_{L_2 L_2'}\sum_{n'\neq n} X_{LL_2'}^{nn'} i^{l_2} B_{L_2}^{(n')}(S_{L_2' L_2}^{(n')} - \delta_{L_2 L_2'})/2i \tag{9}$$

for the incident amplitude $B_L^{(n)}$ on each scatterer n (no external wave, only internal Bloch waves) where $X_{LL_2'}^{nn'}$ is a kernel describing the multiple scattering part between n' and n through a sum over all angular momenta L_1 involving the $C_{L_1,L,L_2'}$ coefficients, spherical harmonics, and spherical Hankel functions of the first kind $h_{L_1}^{(1)}(\kappa R_{nn'})$; $R_{nn'}$ is the distance between the two scatterers n and n'. For a crystal with a single centrosymmetric scatterer per unit cell, $(S_{L'L}^{(n')} - \delta_{LL'})/2i = e^{i\delta_l}\sin(\delta_l)\delta_{LL'}$, and putting $i^l B_L^{(n)} = \tilde{B}_L^{(n)} = \tilde{B}_L e^{i\vec{k}\cdot\vec{R}_n}$ where $\vec{R}_n$ defines the position of the scatterer n (each atom sees an amplitude $B_L e^{i\vec{k}\cdot\vec{R}_n}$ within the Bloch wave), one gets

$$\tilde{B}_L = \sum_{L'}\sum_{n\neq 0} X_{LL'}^{0n} e^{-i\vec{k}\cdot\vec{R}_{0n}} e^{i\delta_{l'}}\sin(\delta_{l'})\tilde{B}_{L'} \tag{10}$$

which becomes in matrix form

$$(I - \mathfrak{X}\Delta)\tilde{B} = 0 \tag{11}$$

with

$$\mathfrak{X}_{LL'} = \sum_{n\neq 0} X_{LL'}^{0n} e^{-i\vec{k}\cdot\vec{R}_{0n}} \quad \text{and} \quad \Delta_{LL'} = e^{i\delta_{l'}}\sin(\delta_{l'})\delta_{LL'}. \tag{12}$$

The nontrivial solution to Eq. (11) implies $|I-\mathfrak{X}\Delta|=0$ or $|\Delta^{-1}-\mathfrak{X}|=0$ in which $(\Delta^{-1})_{LL'}=[e^{-i\delta_l}/\sin(\delta_l)]\delta_{LL'}$ $=[\cot(\delta_l)-i]\delta_{LL'}$. Writing $C_{LL'}=\cot(\delta_l)\delta_{LL'}$, one obtains $|C-iI-\mathfrak{X}|=0$ which, multiplied by κ, yields

$$|\kappa C + \bar{\Gamma}| = 0, \tag{13}$$

where

$$\bar{\Gamma} = -\kappa(iI + \mathfrak{X}). \tag{14}$$

Equation (13) is nothing but Eq. (3). We have thus found the connection between the multiple scattering theory and the KKR method.

With noncentro symmetric scatterers, the scattering matrix is no longer diagonal. Defining the T matrix by $T_{LL'}=(S_{LL'}-\delta_{LL'})$, one finds

$$\tilde{B}_L = \frac{1}{2i}\sum_{L'}\sum_{L_1}\mathfrak{X}_{LL_1}T_{L_1L'}\tilde{B}_{L'} \tag{15}$$

which, in matrix notation, can be written as

$$\left[I - \frac{1}{2i}\mathfrak{X}T\right]\tilde{B} = 0. \tag{16}$$

Following the steps leading to Eq. (14), we finally get

$$|i\kappa(I + 2T^{-1}) + \bar{\Gamma}| = 0. \tag{17}$$

This is the generalization of Eq. (3) for arbitrary scatterers. Note that $i(I+2T^{-1})$ is the inverse of the K matrix.

B. Generalization to many scatterers per unit cell

Segall [36] has generalized the KKR to complex crystals with more than one molecule per unit cell. The idea is to introduce a subcell index j for each scatterer forming the basis of the unit cell such that $\vec{R}_n \to \vec{R}_{n,j}=\vec{R}_n+\vec{\rho}_j$ (here $\vec{\rho}_j$ locates the jth molecule within the unit cell), $T_{LL'}\to T_{LL'}^j\delta_{jj'}$, $K_{LL'}\to K_{LL'}^j\delta_{jj'}$, $\tilde{B}_L^{(n)}\to\tilde{B}_L^{(n,j)}$, $X_{LL'}^{nn'}\to X_{LL'}^{nj,n'j'}$, $\mathfrak{X}_{LL'}\to\mathfrak{X}_{LL'}^{jj'}$, $\bar{\Gamma}_{LL'}\to\bar{\Gamma}_{LL'}^{jj'}$. The Bloch functions satisfy $\tilde{B}_L^{(n,j)}=\tilde{B}_L^j e^{i\vec{k}\cdot\vec{R}_n}$ and

$$|i\kappa K^{-1} + \bar{\Gamma}| = 0. \tag{18}$$

The difference with Eq. (17) resides in the dependence on the index j of the different parameters. One has

$$\bar{\Gamma}^{jj'}_{LL'} = 4\pi i^{l-l'} \sum_{L_1} i^{-l_1} D^{jj'}_{L_1} C_{L_1,L,L'}, \tag{19}$$

where $D^{jj}_{L_1} = D_{L_1}$ as before, whereas

$$D^{jj'}_{L_1} = \tilde{D}^{jj'(1)}_{L_1} + \tilde{D}^{jj'(2)}_{L_1}, \quad j \neq j', \tag{20}$$

with

$$\tilde{D}^{jj'(1)}_{L_1} = \frac{4\pi}{\Omega_m} \frac{i^{l_1}}{\kappa^{l_1}} \sum_p \frac{k_p^{l_1} e^{i\vec{K}_p \cdot (\vec{\rho}_j - \vec{\rho}_{j'})} Y^*_{L_1}(\hat{k}_p)}{\kappa^2 - k_p^2} \exp[(\kappa^2 - k_p^2)/\eta], \tag{21}$$

$$\tilde{D}^{jj'(2)}_{L_1} = -\pi^{-1/2} \frac{2^{l_1+1}}{\kappa^{l_1}} \sum_n e^{i\vec{k}\cdot\vec{A}_{j,j',n}} |\vec{A}_{j,j',n}|^{l_1} Y^*_{L_1}(\hat{A}_{j,j',n}) \times \int_{\sqrt{\eta}/2}^{\infty} d\xi \xi^{2l_1} \exp\left[-\xi^2 |\vec{A}_{j,j',n}|^2 + \frac{\kappa^2}{4\xi^2} \right], \tag{22}$$

and $\vec{A}_{j,j',n} = \vec{A}_n - (\vec{\rho}_j - \vec{\rho}_{j'})$.

IV. RESULTS

A. Cutoff in dipole range

When applying the method described above, one has to be careful with molecules, such as H_2O, which have a dipole moment. Due to its very long range, the dipole leads to very large and even divergent scattering cross sections at low energy. In the philosophy of a muffin-tin approach, all interactions are of finite range. A cutoff in the range of action of the dipole must then be introduced. One might think that it should be cutoff at the radius of the muffins, 2.6 a.u. for the ice structure we are studying [23], as one would normally do with the polarization energy of a centrosymmetric atom. But this is far from obvious since the dipole energy $E_{\text{dip}} = -2\vec{d}\cdot\hat{r}/r^2$ Ry is angle dependent and there can be no matching of the potential energy of the scatterer with the flat V_0 between muffins as one would expect of traditional KKR calculations. Removing the dipole field for $r > a_c$, where a_c is a cutoff radius, is done at the cost of introducing a discontinuity $-2\vec{d}\cdot\hat{r}/a_c^2$ at the muffin edge. As a_c decreases, more dipole is removed but the discontinuity increases. There is hopefully a trade off at some intermediate value of a_c at which the scattering reasonably represents that of the core of the water molecule while minimizing the mismatch. Admittedly, this is far from obvious. What we are then proposing is to find the best value of a_c at which a multiple scattering approach for ice will yield a decent band structure. This preserves the spirit of the KKR which plays a technical support role in the summation of the multiple scattering information contained in $\mathfrak{X}$ and thus $\bar{\Gamma}$ to infinity.

We can illustrate these ideas by showing the total elastic cross section of the H_2O molecule for several different cut off values for the dipole interaction. All the cross sections were calculated with a radius $a = 6$ a.u.. Then a propagation, using the dipole field in the procedure outlined in Eqs. (1) and (2) of Ref. [37], to five different a_c values ranging from 2.6 a.u., that is the half distance between nearest water molecules, to 10 a.u. was performed. This propagation has the approximate effect of adding or subtracting the dipole interaction in the region between a and a_c. Figure 1 shows these cross sections. For $a_c = 10$, and even for $a_c = 8$, the cross sections still display at low energies the behavior that is expected for a dipole driven collision. Use of these radii would therefore imply the inclusion of a significant amount of the dipole interaction, against the premises of the method which does away with the overlapping electron scattering potentials in the condensed phase. The cross sections for $a_c = 2.6$ and 4, on the other hand, are appreciably smaller than those of the other values at the higher energies. This is somewhat unsatisfying in the context of the KKR or the sibling theory of LEED [38] since the propagation to smaller radii should affect mostly the low-energy part [39]. This would indicate that these may similarly not be the best a_c values to employ. We shall see that we get correct energy-band behavior in this whole range of a_c values: it is therefore not possible to exclude forthright any values in this range. Only through a close comparison with experimental data can a selection be made. The analysis we have just done can, after the fact, shed some light on the reason why the midrange values are privileged. Its use as a predictive tool, at least in as much as allowing us to restrict the range of a_c values to be tested, cannot be ascertained from the treatment of a single system.

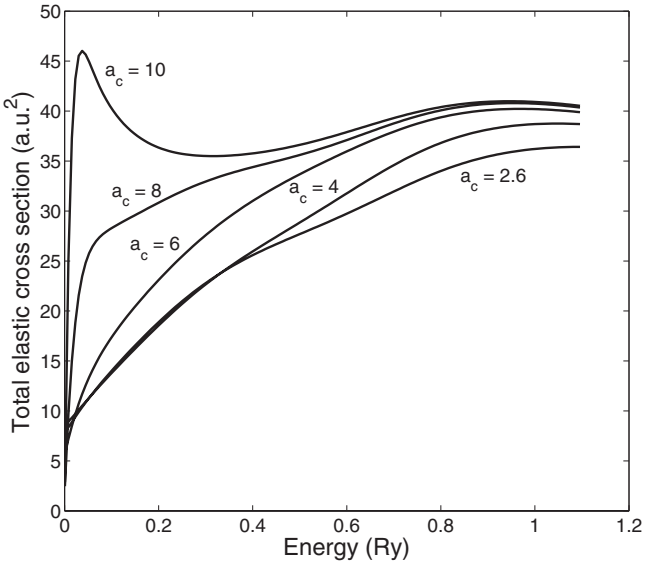

FIG. 1. Total elastic cross section for electron-gas phase H_2O collisions for different values of the cutoff radius a_c.

B. KKR calculations

The ferroelectric cubic phase of ice has a face-centered cubic crystal structure with two H_2O molecules per unit cell. It is well described by Parravicini and Resca [23]. The $D^{jj'}_{L_1}$

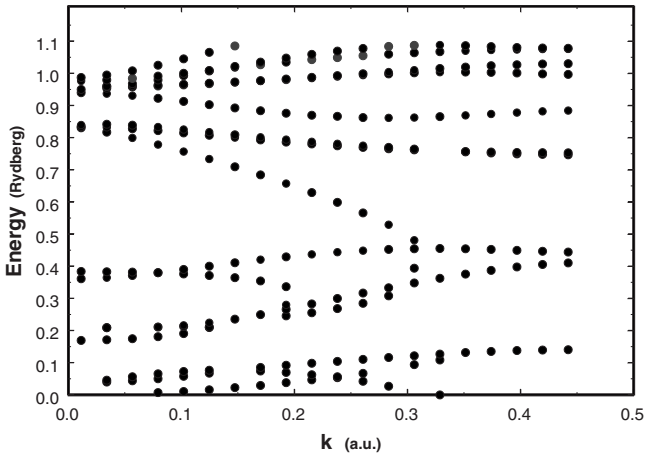

FIG. 2. Bloch eigenmode energy as a function of the wave number in the [111] crystal direction for *R*-matrix data from a partial wave expansion up to $l \leq 4$ using $a_c = 6$ a.u.

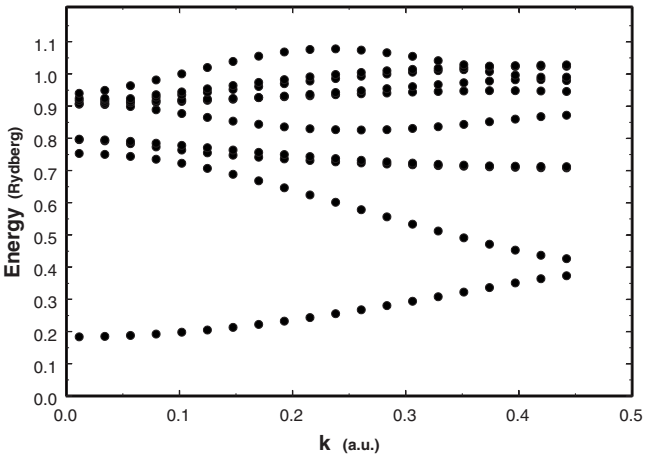

FIG. 3. Bloch eigenmode energy as a function of the wave number in the [111] crystal direction for *R*-matrix data obtained restricting the partial wave expansion to $l \leq 2$ and using $a_c = 6$ a.u.

coefficients are calculated using the structural information of ice given in Parravicini and Resca's paper. Care is taken to properly rotate the scattering matrix, and thus $K^{-1}_{jLL'}$, from the *R*-matrix coordinates to the corresponding position j in the unit cell. The H_2O molecules have their dipoles in the $\hat{z}$ direction in our *R*-matrix calculation which is the common direction chosen in the ferroelectric phase. The two molecules in the unit cell should then be rotated by an angle $\gamma = \pm \pi/4$ around this direction. This is done by using the rotation matrix

$$W_{l,m,l,m'} = e^{-i\gamma m}\delta_{mm'} \tag{23}$$

(see Ref. [40]) on the K matrix

$$\tilde{K} = WKW^{-1}. \tag{24}$$

Note that the tetrahedral symmetry around each molecule of the cubic ice form studied is not strictly respected by the hydrogen in this procedure, but nearly so.

Technically, we have looked for the significant zeros of the determinant (18) at any of 20 given wave numbers k in the crystal [111] direction within the first Brillouin zone. We do an energy sweep using 1000 energy values between 0 and 15 eV. We look for sign changes in the determinant and make sure the minimal eigenvalue of the coefficient matrix goes smoothly through zero. We also take care to eliminate poles (see the structure of $D_L^{(1)}$ and $\tilde{D}_L^{jj'(1)}$).

Figure 2 shows the Bloch eigenmode energies using the full R-matrix angular momentum basis $l \leq 4$ and a cutoff radius of $a_c = 6$ a.u. This has little in common with what one expects of a band structure for energies less than, say, 0.5 Ry. But the upper part is consistent with the work of Ching *et al.* [25], their Fig. 1(a), 12–16 eV range in the ΓL direction. When we do a similar calculation, this time restricting the angular momenta to $l \leq 2$, we discover a very credible band structure as seen in Fig. 3. It compares extremely well with the Ching *et al.* conduction band in their 6–12 eV range. But the upper energy bands are not as well described as in the previous situation; the negative curvature of the uppermost band with band crossing around $k = 0.35$ is incorrect. We have repeated the calculations with this reduced angular momentum basis and a_c ranging from 2.6 a.u. to 10 a.u. The lower energy bands are always well described. The effective mass m^* and the energy E_{CB} at the bottom of the conduction band, where the energy is given by $k^2/m^* + E_{CB}$ Ry, change appreciably as a function of a_c. Figure 4 shows the results. At larger a_c, spurious very-low energy modes appear because of the too large dipole contribution. The estimates for the effective mass vary between 0.8 and 1.0 [41]. The more reliable one [42], which fits the experimental scattering measurements in amorphous ice, gives $m^* = 0.8$. This is very satisfying, well within our range of values and very close to the value $a_c = 6$ a.u. which was selected as being the one yielding the most plausible cross section. One could thus select $a_c = 6.5$ a.u. as yielding the

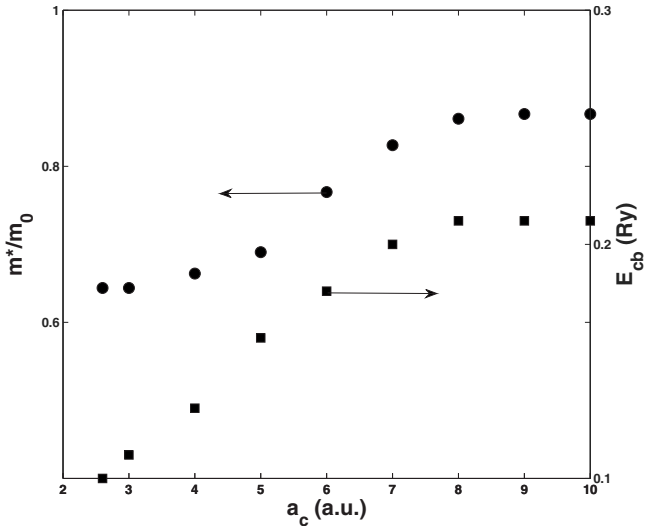

FIG. 4. Effective mass m^* in terms of the free electron mass m_0, circles, and energy E_{CB}, squares, at the bottom of the conduction band as a function of the cutoff radius a_c, i.e., the range of the dipole field.

best fit to experimental data. We can conclude that the dipole cutoff distance does not seem to be critical as there is a very wide range of values for which there is an acceptable band structure. However a calibration based on the effective mass enables a proper selection. It is quite interesting to note that our band structure is highly similar (width of the conduction band, comblike splitting at the higher energy) to the calculation of Ching *et al.* This is probably because they have used a modern first-principles self-consistent orthogonalized linear combinations of atomic orbitals method in the local density approximation. Finally, we have estimated the average polarization energy

$$E_{\mathrm{pol}} \approx \int_{\substack{\text{unit cell} \\ \notin \text{ muffins}}} dV \sum_n (-\alpha/|\vec{r}-\vec{R}_n|^4) \Bigg/ \int_{\substack{\text{unit cell} \\ \notin \text{muffins}}} dV \tag{25}$$

an electron feels between the muffin tins using the experimental value for the polarizability α of 10.13 (a.u.)^3 [43]. We find $E_{\mathrm{pol}} \approx -0.25$ Ry. Adding this reference energy to $E_{CB} \approx 0.19$ Ry at $a_c = 6.5$ a.u. (the dipolar energy averages out to zero), we estimate the bottom of the conduction band to be at roughly −0.06 Ry relative to vacuum. This is in very good agreement with the estimate of −0.75 eV of Ref. [41]. It is instructive to compare these findings with those at $a_c = 2.6$. Not only do we find that the upper band structure conserves the look of the upper part of Fig. 3 even for $l \leq 4$, but the bottom of the conduction band would also be at −0.15 Ry, a much too negative value. This confirms our initial intuition derived from the elastic cross section.

V. DISCUSSION

Now, how can one understand the need to restrict the low-energy calculations to $l \leq 2$? This has to do with the angular momentum energy barrier $E(l,r) = l(l+1)/r^2$ Ry that an electron sees when approaching a molecule with an angular momentum l. Only electrons with kinetic energy E_e larger that $E(l,r)$ will get closer than r to the scatterer. Thus, any electron of energy E_e undergoing multiple scattering between two molecules a distance d_m apart will only be able to do so for those values of l such that $E(l,d_m) < E_e$. This can also be examined from a semiclassical point of view. For an electron with angular momentum $L \sim kr$, one can write $L^2 \approx l(l+1) = k^2 r^2$. It is only for $r \lesssim d_m$ that two molecules can exchange information through the electron since it is otherwise outside their reach. This means that the relevant angular momenta are those for which $l(l+1)/k^2 = l(l+1)/E_e \lesssim d_m^2$. This is consistent with what we see in our results.

Let us put some numbers on this condition. For cubic ice, $d_m \approx 5.2$ a.u. and $E(3,d_m) = 0.44$ Ry. This means that in the energy range $E_e < 0.44$ Ry, one can only have $l \leq 2$. But then, $E(5,d_m) = 1.11$, which explains why the band structure for $l \leq 4$ should be better at the upper energies.

We have just mentioned physical arguments for the angular momentum cutoff. But what is the mathematical reason? Let us go back to Eq. (18) or its multiple scattering equivalent (16) which is easier to analyze. It turns out that $\bar{\Gamma}$ and $\mathfrak{X}$ become quite divergent for large values of angular momenta at low energy. As mentioned previously, $\mathfrak{X}_{LL'}^{ij'}$ involves a sum over L_1 of the spherical Hankel function of the first kind $h_{L_1}^{(1)}(\kappa R_{nn'})$. This Hankel function diverges as $(\kappa R_{nn'})^{-(l_1+1)}$ for small values of its argument $(\kappa R_{nn'})$. The singular behavior is obviously dominated by the nearest-neighbor distance d_m. For $l=4$, l_1 can be as large as $2l=8$ [see Eq. (4)]. So even though one expects the $l=4$ components of the K and T matrices to get smaller as the energy decreases, it is the product $\mathfrak{X}T$ in Eq. (16) which is ill behaved because of the predominance of the Hankel function.

We should mention that we are currently applying these multiple collision ideas on a H_2O dimer [44]. We are able to produce a cross section that is within 5% of the one calculated with a full R-matrix treatment for energies larger than 2.5 eV. This covers the range of energies encountered in our present band calculations.

In conclusion, we have found that the R-matrix gas phase elastic scattering data can be used in cubic ice to reasonably reproduce its electronic band structure. A proper value of the cutoff radius must be determined which leads to a physically significant K matrix that respects the spirit of the KKR. Two cutoffs have to be applied. The first one is on the range of the molecular dipole. The second cutoff on angular momentum depends on both the energy and the intermolecular distance. Strictly speaking, only values $l \leq l_o$ should be retained such that $E(l_o,d_m) < E_e < E(l_o+1,d_m)$ although our dimer calculations indicate that there is some flexibility in its application. The effective reach of the molecules passes through this angular momentum cutoff in addition to the R-sphere radius. These findings should also apply in condensed phases with other molecular constituents. Ideally, a calibration on a crystalline phase should be attempted provided reliable experimental or theoretical values are available for the electron states. With the trimmed T-matrix, one could make computationally efficient large cluster calculations which include multiple scattering and extract useful information on cross sections, in a fashion similar to the approach in Ref. [20], for instance.

[1] S. M. Pimblott and J. A. LaVerne, J. Phys. Chem. A **102**, 2967 (1998).
[2] L. Sanche, Radiat. Phys. Chem. **32**, 269 (1988).
[3] D. T. Goodhead, P. O'Neill, and H. G. Menzel, *Microdosimetry* (The Royal Society of Chemistry, Cambridge, UK, 1997).
[4] *Photon, Beam, and Plasma Stimulated Chemical Processes at Surfaces*, edited by V. M. Donnelly, I. P. Herman, and M. Hirose, (Materials Research Society, Pittsburg, PA, 1987).
[5] R. D. Ramsier and J. T. Yates, Jr, Surf. Sci. Rep. **12**, 243 (1991), and references therein.

[6] *Desorption Induced by Electronic Transitions–DIET III*, Vol. 13 of Springer Series in Surface Sciences (Springer-Verlag, Berlin, 1988).
[7] T. D. Harris, D. H. Lee, M. Q. Blumberg, and C. R. Arumainayagam, J. Phys. Chem. **99**, 9530 (1995).
[8] *Laser Spectroscopy and Photochemistry on Metal Surfaces* edited by D. T. Goodhead, P. O'Neill, and H. G. Menzel (World Scientific, Singapore, 1995).
[9] *Energetic Charged-particle Interactions with Atmospheres and Surfaces*, Vol. 19 of Physics and Chemistry in Space (Springer-Verlag, Berlin, 1988).
[10] L. Sanche, IEEE Trans. Dielectr. Electr. Insul. **4**, 507 (1997).
[11] J. Lekner, Phys. Rev. **158**, 130 (1967).
[12] L. Sanche, A. D. Bass, P. Ayotte, and I. I. Fabrikant, Phys. Rev. Lett. **75**, 3568 (1995).
[13] I. I. Fabrikant, K. Nagesha, R. Wilde, and L. Sanche, Phys. Rev. B **56**, R5725 (1997).
[14] K. Nagesha, I. I. Fabrikant, and L. Sanche, J. Chem. Phys. **114**, 4934 (2001).
[15] I. I. Fabrikant, Phys. Rev. A **76**, 012902 (2007).
[16] W. M. Huo and F. A. Gianturco, *Computational Methods for Electron-Molecule Collisions* (Plenum, New York, 1995).
[17] P. G. Burke and K. A. Berrington, *Atomic and Molecular processes: An R-matrix Approach* (Institute of Physics Publishing, Bristol, 1993).
[18] D. Teillet-Billy, D. T. Stibbe, J. Tennyson, and J. P. Gauyacq, Surf. Sci. **443**, 57 (1999).
[19] D. C. Marinica, D. Teillet-Billy, J. P. Gauyacq, M. Michaud, and L. Sanche, Phys. Rev. B **64**, 085408 (2001).
[20] D. C. Marinica, D. Teillet-Billy, and J. P. Gauyacq, Phys. Rev. B **71**, 115438 (2005).
[21] P. Andreo, Phys. Med. Biol. **36**, 861 (1991).
[22] J. Meesungnoen, J.-P. Jay-Gerin, A. Filali-Mouhim, and S. Mankhetkorn, Radiat. Res. **158**, 657 (2002).
[23] G. P. Parravicini and L. Resca, Phys. Rev. B **8**, 3009 (1973).
[24] L. Resca and R. Resta, Phys. Status Solidi B **81**, 129 (1977).
[25] W. Y. Ching, L. Liu, and Y.-N. Xu, Ferroelectrics **153**, 25 (1994).
[26] J. Tennyson and L. A. Morgan, Philos. Trans. R. Soc. London, Ser. A **357**, 1161 (1999).
[27] A. Faure, J. D. Gorfinkiel, L. A. Morgan, and J. Tennyson, Comput. Phys. Commun. **144**, 224 (2002).
[28] J. D. Gorfinkiel, L. A. Morgan, and J. Tennyson, J. Phys. B **35**, 543 (2002).
[29] T. H. Dunning, J. Chem. Phys. **53**, 2823 (1970).
[30] T. H. Dunning, J. Chem. Phys., **55**, 716 (1971).
[31] G. C. Fletcher, *The Electron Band Theory of Solids* (North-Holland, Amsterdam, 1971).
[32] L. G. Caron and L. Sanche, Phys. Rev. Lett. **91**, 113201 (2003).
[33] L. Caron and L. Sanche, Phys. Rev. A **70**, 032719 (2004).
[34] L. Caron and L. Sanche, Phys. Rev. A **72**, 032726 (2005).
[35] B. Segall and F. S. Ham, in *Energy Bands of Solids*, edited by B. Alder, S. Fernbach, and M. Rotenberg Vol. 8 of Methods in computational physics (Academic, New York, 1968) p. 251.
[36] B. Segall, Phys. Rev., **105**, 108 (1957).
[37] K. L. Baluja, P. G. Burke, and L. A. Morgan, Comput. Phys. Commun. **27**, 299 (1982).
[38] J. Pendry, *Low Energy Electron Diffraction* (Academic, London, 1974).
[39] M. Michaud, L. Sanche, C. Gaubert, and R. Baudoing, Surf. Sci. **205**, 447 (1988).
[40] A. Messiah, *Quantum Mechanics* (Wiley, New York, 1962).
[41] A. Bernas, C. Ferradini, and J.-P. Jay-Gerin, Chem. Phys. **222**, 151 (1997).
[42] M. Michaud, A. Wenn, and L. Sanche, Radiat. Res. **159**, 3 (2003).
[43] T. N. Olney, N. M. Cann, G. Cooper, and C. E. Brion, Chem. Phys. **223**, 59 (1997).
[44] D. Bouchiha, J. D. Gorfinkiel, L. G. Caron, and L. Sanche (unpublished).